

Magnetic Properties of Fe₃O₄ Films on Fe(001)

M. ZAJĄC^{a,*}, D. AERNOUT^a, K. FREINDL^b, K. MATLAK^a,
N. SPIRIDIS^b, M. ŚLĘZAK^a, T. ŚLĘZAK^a AND J. KORECKI^{a,b}

^aFaculty of Physics and Applied Computer Science

AGH University of Science and Technology

Al. Mickiewicza 30, 30-059 Kraków, Poland

^bInstitute of Catalysis and Surface Chemistry, Polish Academy of Sciences

Niezapominajek 8, 30-239 Kraków, Poland

We investigated the magnetic properties of ultrathin magnetite films deposited directly on MgO(001) and on a Fe(001) buffer layer. In both cases the magnetite surface structure could be identified using low energy electron diffraction. The conversion electron Mössbauer spectroscopy measurements proved that, for magnetite films deposited on the Fe buffer, superparamagnetic relaxation was strongly suppressed. The effect of a Fe overlayer on the magnetite film grown directly on MgO is considerably weaker. Longitudinal Kerr magnetometry indicated the presence of the ferromagnetic interfacial coupling between Fe and magnetite films. We conclude that the density of antiphase boundaries for films grown on the Fe buffer is lower than that of Fe₃O₄/MgO films.

PACS numbers: 75.75.+a, 76.80.+y

1. Introduction

For many years magnetite has attracted attention from theoretical and technological points of view. Its importance arises from its interesting electronic and magnetic properties. It is ferrimagnetic with a high Curie temperature (858 K) and thus possesses a net magnetization at room temperature. Moreover, it is conducting, which is rather exceptional among oxides, and because the Fermi level lies in the minority band, a large spin polarization of conduction electrons is obvious. This makes magnetite favourable for spintronic applications. Most spintronic devices are based on thin film technology. Unfortunately, due to subtle structural peculiarities typical of epitaxial growth, the magnetic properties of magnetite films

*corresponding author; e-mail: mzajac@uci.agh.edu.pl

are strongly different from the bulk material and depend on the layer thickness. It is believed that many of these differences are related to an antiphase domain structure [1–3] formed in the films during their growth. Magnetite grows on MgO(100) in a layer-by-layer mode, and the first step of the growth mechanism is the formation of nuclei, followed by growth and eventual coalescence of two-dimensional islands into a closed layer [3]. The oxygen sublattice remains undisturbed across the MgO/Fe₃O₄ interface, but the iron sublattices in the neighbouring islands can be shifted and rotated with respect to each other due to the different symmetries and lattice parameters of magnesium oxide and magnetite. When the islands coalesce, antiphase boundaries (APBs) form between them, as revealed by scanning tunneling microscopy (STM) [4]. The first transmission electron microscopy (TEM) pictures of APBs in epitaxial magnetite films, which allow the determination of the APB density, were reported by Margulies et al. [1] for a 50 nm thick sample grown by sputter deposition at 770 K, showing domains that were, on average, 27.5 nm wide. For oxygen assisted MBE at a growth temperature of 500 K, Hibma et al. [3] reported APBs that are an order of magnitude larger. This large difference is probably connected to the very different preparation conditions, which modify the nucleation density of Fe₃O₄ islands.

The presence of APBs strongly influences the magnetic properties of magnetite. Most of all, Fe₃O₄ ultrathin films show superparamagnetic behaviour [2, 5], which is the most critical effect hindering potential applications of ultrathin magnetite films. Furthermore, antiferromagnetic coupling between antiphase domains across the APBs results in a higher saturation magnetic field observed for thin magnetite films as compared to the bulk crystal [1, 6], and consequently, despite the magnetic shape anisotropy, the local magnetic moments in the Fe₃O₄ layers are not oriented in the film plane [2, 6].

One of the potential ways of removing unwanted effects originating from the antiphase domain structure is to select an appropriate substrate material and its crystallographic orientation. Eerenstein et al. [7] used a MgAl₂O₄ instead of a MgO substrate, resulting in the formation of larger domains and a shift of the superparamagnetic limit to a lower thickness.

In our report, we describe another possibility, relying on the presence of an iron overlayer or a buffer layer between the substrate and the magnetite film. It is shown that properties of magnetite films grown on a ferromagnetic substrate are modified, not only due to a different character of the epitaxial growth, but also by the exchange interaction occurring at the Fe/Fe₃O₄ interface.

2. Experiment and results

The experiment was performed using a multi-chamber ultrahigh vacuum (UHV) system (base pressure 1×10^{-10} mbar). A preparation chamber contains a miniature MBE system, consisting of metal vapour sources, quartz monitors to control the evaporation rate and a four-grid electron spectrometer. Next to the

preparation chamber, there is a small chamber enabling *in situ* magneto-optic Kerr effect (MOKE) measurements. A separate chamber is dedicated to *in situ* conversion electron Mössbauer spectroscopy (CEMS) using a large opening channeltron as a detector. The sample was mounted to a cold finger of a stationary liquid nitrogen cryostat, which allowed measurements over a temperature range between 80 K and 500 K. All the samples were prepared on MgO(001) substrates cleaved in N_2 atmosphere prior to their introduction into the UHV system. The substrates were then annealed for 1 h at 900 K in UHV. Then, the MgO(001) surface showed atomic cleanliness and perfect structural order, as verified by the Auger electron spectroscopy and low energy electron diffraction (LEED). Magnetite was grown by Fe-vapour deposition at a rate of approximately 1 nm/min in the presence of oxygen, provided by a precision leak valve. The combination of ^{56}Fe and ^{57}Fe isotopes used during the sample preparation allowed for selective Mössbauer studies of magnetite films. For the substrate held at 520 K, the magnetite phase could be stabilized in a broad range of the O_2 partial pressure ($1 \times 10^{-7} \div 1 \times 10^{-6}$ hPa).

First, a 25 Å thick epitaxial $^{57}Fe_3O_4(001)$ layer on the MgO(001) substrate was investigated. The LEED patterns of the oxide surface displayed a $(\sqrt{2} \times \sqrt{2})R45^\circ$ reconstruction relative to the primitive surface unit cell of magnetite. This type of reconstruction is typical of the (001) surface of bulk magnetite crystals [8], as well as of the surface of epitaxial magnetite films on MgO(001) [4, 9–11]. The magnetic properties were checked *in situ* by CEMS. The Mössbauer spectrum shown in Fig. 1a, similar to that obtained in previous experiments [2, 5], is characteristic of superparamagnetic (spm) relaxation. The spectrum was fitted using the Blume–Tjon model [12] of relaxation, including a narrow distribution of the fluctuation frequency and averaged hyperfine parameters of magnetite (hyperfine magnetic field $B_{hf} = 46.0$ T and isomer shift $IS = 0.36$ mm/s). The best fit was obtained for the average fluctuation frequency of $\Omega = 95$ MHz and for a small magnetic polarization of the spm assembly corresponding to $m = 0.16$ of the saturation magnetization. Such a polarization was always observed in our CEMS measurements of ultrathin magnetite films, and we explain it as resulting from the coupling between the antiphase domains [13]. At 80 K, the spm fluctuations slow down and the CEMS spectrum [14] becomes typical of the magnetite phase below the Verwey transition, which, in combination with the LEED pattern, allowed us to identify the obtained oxide film as magnetite.

After the CEMS measurement, a 50 Å iron layer was deposited at room temperature on the magnetite film. To selectively monitor the effect of a ferromagnetic overlayer on the spm properties of the ultrathin magnetite film, we used the ^{56}Fe isotope that did not contribute to the CEMS spectrum. The ^{56}Fe overlayer makes the spectrum of the oxide film beneath much more complex (Fig. 1b). First of all, it shows a distinct magnetic splitting, which means that the spm fluctuations are partially suppressed. However, the best fit was still obtained using relaxation components combined with the two static ones. To account for the relaxation be-

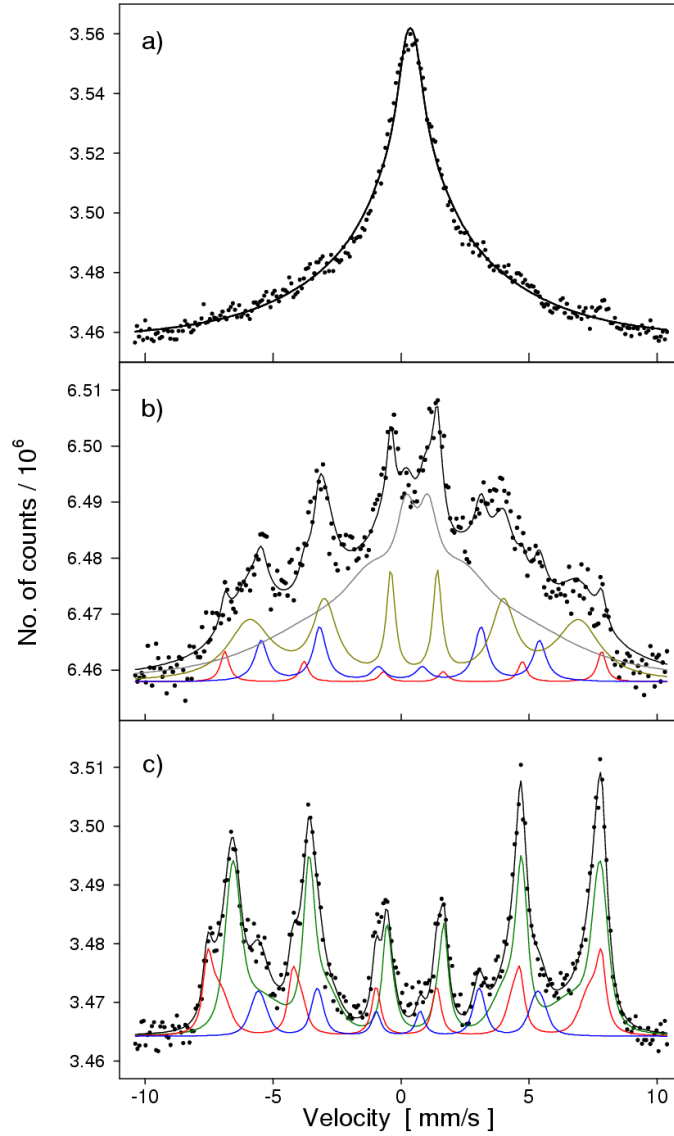


Fig. 1. CEMS spectra of the 25 Å ⁵⁷Fe₃O₄ layer (a) and of 50 Å ⁵⁶Fe/25 Å ⁵⁷Fe₃O₄ (b) and 25 Å ⁵⁷Fe₃O₄/200 Å ⁵⁶Fe (c) bilayers prepared on the MgO(001) cleaved substrate.

haviour, it was necessary to introduce two spectral components. The first one was very similar to that describing the film before it was coated with Fe ($\Omega = 90$ MHz, $m = 0.36$), while the second one, with the same Ω , was characterized by a much higher polarisation $m = 0.77$, which is equivalent to a magnetic field acting on a part of the magnetite film. We postulate that the 50 Å Fe film magnetically biases an interfacial part of the oxide layer and that the effect is analogous to that

induced by the external magnetic field on spm particles [15]. Beside these two relaxation components, the numerical analysis of the CEMS spectrum measured for the $MgO/^{57}Fe_3O_4/^{56}Fe$ system indicated the presence of a phase with parameters very close to metallic iron ($B_{hf} = 33.3$ T, $IS = 0.02$ mm/s relative to α -Fe), which proves the exchange of interfacial $^{57}Fe/^{56}Fe$ atoms during deposition of the ^{56}Fe overlayer. A further increase in the iron film thickness (up to 100 Å) did not change magnetic properties of the magnetite layer.

Next, we investigated the role of the iron buffer layer by studying magnetic properties of the epitaxial $Fe_3O_4(001)/Fe(001)$ bilayer grown on $MgO(001)$. We have recently shown [16] that the structural quality of the magnetite films on the $Fe(001)$ buffer is superior to those grown directly on MgO , mainly due to a higher applicable post-preparation annealing temperature. The preparation of the 200 Å thick epitaxial $^{56}Fe(001)$ buffer layer on $MgO(001)$ was optimized to obtain atomically flat films. On the iron layer, a 25 Å thick oxide layer was grown using ^{57}Fe , in the same way as it was done on MgO , but after the deposition the sample was annealed for 1 hour at 770 K under UHV conditions. The LEED patterns showed the $(\sqrt{2} \times \sqrt{2})R45^\circ$ reconstruction that is typical of magnetite.

A room temperature CEMS spectrum measured *in situ* for the $^{57}Fe_3O_4(001)/^{56}Fe(001)/MgO$ bilayer is shown in Fig. 1c. The spectrum is completely different to that of the $Fe_3O_4(001)/MgO$. Sharp and well-resolved lines reflect the static characteristic of the spectrum. The spm relaxation is totally suppressed. The best spectrum fit could be obtained by assuming three types of iron sites labelled by their isomer shifts. Two of them are representative for magnetite, corresponding to Fe^{3+} ions in tetrahedral positions ($IS = 0.30$ mm/s) and octahedral iron ions ($IS = 0.67$ mm/s) with a mixed valency of +2.5 on average. The average hyperfine magnetic fields for the tetrahedral (46.2 T) and octahedral (41.8 T) sites are slightly reduced compared to the bulk magnetite phase. This can be attributed to a surface effect [17] and/or to deviation of the ultrathin magnetite film from the ideal structure and stoichiometry. What is more interesting is the ratio of octahedral to tetrahedral sites, which for bulk magnetite amounts to two and is shifted toward a much higher value (near three). This, to the best of our knowledge, was never observed in bulk or in thin film magnetite-like species. This may be interpreted as a strong deviation from stoichiometry towards FeO , or as an electronic effect involving a charge transfer from the Fe buffer layer to the oxide film. A small (corresponding to about 1.5 monolayers) α - Fe like component originating from the isotope intermixing at the Fe/Fe_3O_4 interface is not surprising, taking into account the high temperature annealing. The slightly enhanced hyperfine magnetic field of the iron phase (33.8 T) can be related to the oxide induced magnetic biasing occurring at the interface.

As mentioned above, the superparamagnetism is affected by a magnetic interaction between magnetite and the iron layer. The coupling between the iron buffer layer and the magnetite overlayer could be observed directly by applying

in situ Kerr magnetometry, subsequently for the Fe and the Fe/Fe₃O₄ bilayer. Longitudinal Kerr loops measured with the magnetic field applied along the easy magnetization direction of Fe(001), corresponding to the [110] in-plane direction of MgO(001), are shown in Fig. 2. In the case of the Fe/Fe₃O₄ bilayer, the MOKE

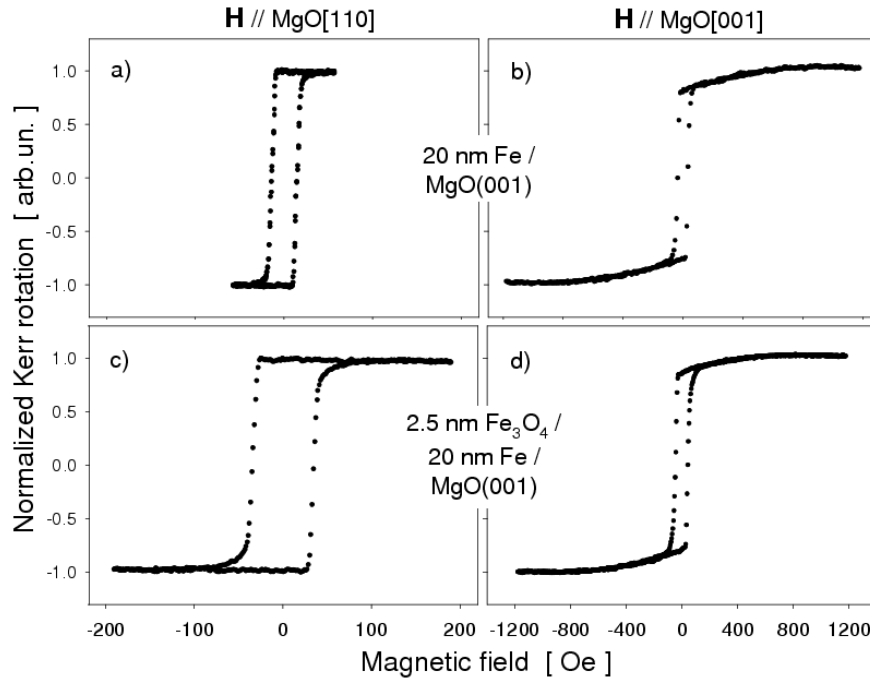


Fig. 2. MOKE hysteresis loops of the 200 nm iron film (a), (b) and of the 25 Å Fe₃O₄/200 Å Fe bilayer (c), (d) measured with the magnetic field along the easy (left column) and hard (right column) magnetization direction.

measurements predominantly probe the magnetization of the Fe buffer due to the large differences between thickness and saturation magnetization of the metallic and oxide layer. The shape of the hysteresis loops for the 200 Å Fe layer (Fig. 2a, b) does not change vitally after adding the 25 Å magnetite film. However, a substantial increase in the coercive field, H_C , is observed, with an $H_C = 13$ Oe observed for the Fe buffer layer and an $H_C = 34$ Oe observed for the Fe/Fe₃O₄ bilayer. The change of the coercive fields suggests weak interfacial ferromagnetic coupling.

3. Conclusions

The proximity of an Fe layer suppresses superparamagnetic behaviour in ultrathin Fe₃O₄(001) films. The role of the Fe overlayer and the buffer layer is different. While the overlayer causes only a weak effect, similar to the influence of

an external magnetic field, the Fe buffer layer entirely suppresses the superparamagnetism. Such an extent of the effect indicates different mechanisms involved in the two cases. We suggest that the magnetite films grown on Fe have a lower density of antiphase domains. This conclusion, confirmed by our preliminary scanning tunnelling microscopy observations [16], should be verified using transmission electron microscopy.

Acknowledgments

This work was partially supported by 6 FP Project “Ultrasmooth”, MRTN-CT-2003-504462.

References

- [1] D.T. Margulies, F.T. Parker, M.L. Rudee, F.E. Spada, J.N. Chapman, P.R. Aitchison, A.E. Berkowitz, *Phys. Rev. Lett.* **79**, 5162 (1997).
- [2] F.C. Voogt, T.T.M. Plastra, L. Niesen, O.C. Rogojanu, M.A. James, T. Hibma, *Phys. Rev. B* **57**, R8017 (1998).
- [3] T. Hibma, F.C. Voogt, L. Niesen, P.A.A. van der Heijden, W.J.M. de Jonge, J.J.T.M. Donkers, P.J. van der Zaag, *J. Appl. Phys.* **85**, 5291 (1999).
- [4] J.M. Gaines, P.J.H. Bloemen, J.T. Kohlhepp, C.W.T. Bulle-Lieuwma, R.M. Wolf, A. Reinders, R.M. Jungblut, P.A.A. van der Heijden, J.T.W.M. van Eemeren, J. aan de Stegge, W.J.M. de Jonge, *Surf. Sci.* **373**, 85 (1997).
- [5] B. Handke, J. Haber, T. Slezak, M. Kubik, J. Korecki, *Vacuum* **63**, 331 (2001).
- [6] D.T. Margulies, F.T. Parker, F.E. Spada, R.S. Goldman, J. Li, R. Sinclair, A.E. Berkowitz, *Phys. Rev. B* **53**, 9175 (1996).
- [7] W. Eerenstein, L. Kalev, L. Niesen, T.T.M. Plastra, T. Hibma, *J. Magn. Magn. Mater.* **258**, 73 (2003).
- [8] G. Tarrach, D. Burgler, T. Schaub, R. Wiesendanger, H.-J. Güntherodt, *Surf. Sci.* **285**, 1 (1993).
- [9] S.A. Chambers, S.A. Joyce, *Surf. Sci.* **420**, 111 (1999).
- [10] S.A. Chambers, S. Thevuthasan, S.A. Joyce, *Surf. Sci.* **450**, L273 (2000).
- [11] B. Stanka, W. Hebenstreit, U. Diebold, S.A. Chambers, *Surf. Sci.* **448**, 49 (2000).
- [12] M. Blume, J.A. Tjon, *Phys. Rev.* **165**, 446 (1968).
- [13] K. Freindl et al., in preparation.
- [14] J. Korecki, B. Handke, N. Spiridis, T. Ślęzak, I. Flis-Kabulska, J. Haber, *Thin Solid Films* **412**, 14 (2002).
- [15] P. Roggwiller, W. Kündig, *Solid State Commun.* **12**, 901 (1973).
- [16] N. Spiridis, J. Barbasz, Z. Łodziana, J. Korecki, *Phys. Rev. B* **74**, 155423 (2006).
- [17] N. Spiridis, B. Handke, T. Ślęzak, J. Barbasz, M. Zając, J. Haber, J. Korecki, *J. Phys. Chem. B* **108**, 14356 (2004).